

## Molybdenum at High Pressure and Temperature: Melting from Another Solid Phase

A. B. Belonoshko,<sup>1,2</sup> L. Burakovsky,<sup>3</sup> S. P. Chen,<sup>3</sup> B. Johansson,<sup>1,4</sup> A. S. Mikhaylushkin,<sup>5</sup> D. L. Preston,<sup>6</sup> S. I. Simak,<sup>5</sup> and D. C. Swift<sup>6</sup>

<sup>1</sup>*Applied Materials Physics, Department of Material Science and Engineering, The Royal Institute of Technology, 10044 Stockholm, Sweden*

<sup>2</sup>*Institute of Theoretical Physics, AlbaNova University Center, The Royal Institute of Technology, 10691 Stockholm, Sweden*

<sup>3</sup>*Theoretical Division, Los Alamos National Laboratory, Los Alamos, New Mexico 87545, USA*

<sup>4</sup>*Condensed Matter Theory Group, Department of Physics, Box 530, Uppsala University, 75121 Uppsala, Sweden*

<sup>5</sup>*Department of Physics, Chemistry and Biology (IFM), Linköping University, 58183 Linköping, Sweden*

<sup>6</sup>*Physics Division, Los Alamos National Laboratory, Los Alamos, New Mexico 87545, USA*

(Received 15 October 2007; published 3 April 2008)

The Gibbs free energies of bcc and fcc Mo are calculated from first principles in the quasiharmonic approximation in the pressure range from 350 to 850 GPa at room temperatures up to 7500 K. It is found that Mo, stable in the bcc phase at low temperatures, has lower free energy in the fcc structure than in the bcc phase at elevated temperatures. Our density-functional-theory-based molecular dynamics simulations demonstrate that fcc melts at higher than bcc temperatures above 1.5 Mbar. Our calculated melting temperatures and bcc-fcc boundary are consistent with the Mo Hugoniot sound speed measurements. We find that melting occurs at temperatures significantly above the bcc-fcc boundary. This suggests an explanation of the recent diamond anvil cell experiments, which find a phase boundary in the vicinity of our extrapolated bcc-fcc boundary.

DOI: [10.1103/PhysRevLett.100.135701](https://doi.org/10.1103/PhysRevLett.100.135701)

PACS numbers: 64.10.+h, 64.70.D-, 64.70.K-, 71.15.Pd

Extensive experimental work [1–6] and many theoretical studies [7–17] of the phase diagram of Mo have been carried out. It has been established both theoretically [15] and experimentally [5] that at low temperatures ( $T$ ) Mo is stable in the bcc phase up to a pressure ( $P$ ) of about 7 Mbar (1 Mbar = 100 GPa), where it transforms to the fcc phase. Sound speed measurements in Mo under shock compression show that the Hugoniot first crosses a phase boundary at  $P = 2.1$  Mbar at an estimated  $T = 4100$  K, and that it crosses a second phase boundary at  $P = 3.9$  Mbar at an estimated  $T = 10\,000$  K [2]. The lower point was interpreted as a bcc-solid transition, while the higher point was assumed to be melting. More recently, Errandonea *et al.* obtained diamond anvil cell (DAC) data on the melting temperature ( $T_m$ ) of Mo to 1 Mbar [6]. Their DAC data are inconsistent with the shock-wave (SW) data [2]. The DAC melting curve has a very small slope— $T_m$  varies from 2900 K at  $P = 0$  to 3100 K at 1 Mbar—which approaches zero at high  $P$ , whereas the SW data imply a mean slope of  $\sim 18$  K GPa<sup>-1</sup> over the  $P$  interval 0–4 Mbar. Extrapolation of the DAC melt curve to 2.1 Mbar gives a melting  $T$  of approximately 3300 K, which is near but somewhat below the transition identified as solid-solid in the SW data. Consequently, Errandonea *et al.* conclude that melting at 2.1 Mbar had been misinterpreted by Hixson *et al.* as a solid-solid transition, and that the high- $P$  transition reported in [2] does not appear to be melting.

On the other hand, there are several reasons to question these conclusions of Errandonea *et al.* First, it is possible that the DAC Mo sample flows, not because of melting, but because of internal nonhydrostatic stresses associated with

a solid-solid phase transformation [18,19]. Also we note that observed or predicted  $T$ -induced solid-solid transitions in a number of materials other than Mo have been reinterpreted by the DAC technique [6] as melting; examples include MgO [20–22], Fe [23–25], and Xe [26,27]. In every case where a DAC melting curve exhibits an unusually low Clapeyron slope, there is independent evidence for a  $T$ -induced solid-solid transition. Quite remarkably, when theory does not predict a solid-solid transition, the theoretical and DAC melting curves are in very good agreement, as is the case for NaCl [20], MgSiO<sub>3</sub> perovskite [28], SiO<sub>2</sub> [29], Al<sub>2</sub>O<sub>3</sub> [30], Al [31], and Cu [32], to name a few. In view of these considerations, it is quite possible that some, if not all, low-slope DAC melting curves are in fact solid-solid phase boundaries. In particular, it is our contention that the DAC melting curve of Mo at high  $P$  is essentially a bcc-solid phase boundary [15], and that the original interpretation of the SW data on Mo [2,4] is correct.

Even though the low- $T$  fcc phase field of Mo lies above 7 Mbar [15], we decided to compute the Gibbs free energies of the fcc and bcc phases over the  $P$  range 0–8 Mbar. The free energies were calculated in quasiharmonic approximation within the framework of the frozen-core all-electron projector augmented wave method [33], as implemented in the Vienna *ab initio* simulation package (VASP) [34]. The energy cutoff was set to 400 eV. Exchange and correlation potentials were treated within the generalized gradient approximation [35]. The semicore  $4p$  states of Mo were treated as valence. The integration over the Brillouin zone (BZ) was based on the Monkhorst-Pack scheme [36],

which specifies a fine grid of  $k$  points in the irreducible part of the BZ. Relaxation procedures and force calculations at zero  $T$  were carried out according to the Methfessel-Paxton scheme [37], while accurate total energy calculations were performed by means of the linear tetrahedron method with Blöchl's correction [38]. All necessary convergence tests were performed; the total and free energies were converged to within 0.5 meV/atom. The convergence of the vibrational free energies of the fcc and bcc structures with respect to the  $k$  point grid and the energy cut-off was attained. The phonon frequency calculations were carried out in the framework of the supercell approach using the small displacement method described in detail in Ref. [39]. To maintain the high accuracy indicated above we used  $3 \times 3 \times 3$  supercells. Forces induced by small atomic displacements were calculated using the VASP program. The free energy was calculated as the sum of the electronic and vibrational contributions. The equation of state was obtained by accurate numerical interpolation of the calculated Helmholtz free energies using the Birch-Murnaghan equation [40].

Under ambient conditions the fcc structure is dynamically unstable, that is, imaginary frequencies are present in its phonon spectrum. Under compression at low  $T$  the imaginary frequencies decrease in magnitude and finally disappear at about 350 GPa ( $V = 10.2 \text{ \AA}^3$ ), indicating that the fcc structure becomes dynamically, though not thermodynamically, stable. In addition, as  $P$  increases from zero, the low- $T$  free energy difference between the bcc and fcc structures smoothly decreases to zero at roughly 7 Mbar. At higher  $P$ , fcc is the more stable structure. It should be stressed that both the bcc and fcc phases are dynamically stable from 350 GPa to the highest  $P$  considered in this Letter, namely, 850 GPa; hence, the free energies can be calculated in the quasiharmonic approximation over this  $P$  range. The difference of the calculated Gibbs free energies is shown in Fig. 1. The corresponding bcc-fcc phase boundary, which consists of two disjoint curves, is displayed in Fig. 2. The fcc structure occupies the lower right region of the figure at  $P > 700$  GPa. The other piece of the bcc-fcc phase boundary running from approximately (400 GPa, 6000 K) to (650 GPa, 7500 K) shows that fcc is more stable than bcc at high  $T$ . This is consistent with our fcc and bcc  $T_m$  calculations described below.

To check whether the relative stability of two solid phases is affected by anharmonism we performed MD simulations of melting of each of the two phases; the structure with the higher  $T_m$  is the more stable phase. We performed *ab initio* molecular dynamics (AIMD) simulations with the same *ab initio* method as described above for the phonon calculations.

The  $T_m$ s of fcc Mo were calculated using the  $Z$  method [41] (we have named it so because of the characteristic  $Z$ -letter shape of the isochore) in the  $NVE$  ( $N$  number of atoms,  $V$  volume,  $E$  energy) ensemble. In the  $Z$  method the

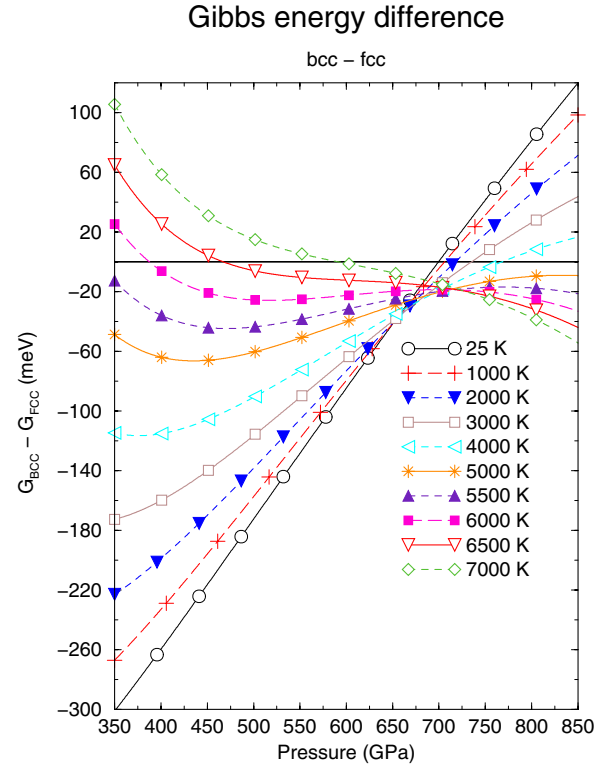


FIG. 1 (color online). The difference of the Gibbs free energies of the bcc and fcc phases of Mo as a function of pressure for several temperatures. A positive difference indicates that the fcc phase is more stable.

initial configuration of the system is solid, and its final state lies on the isochore corresponding to its fixed volume. Such an isochore consists of three pieces: (i) crystalline, which in turn consists of two parts: a solid one, and a superheated solid one that extends into the liquid region of the phase diagram above the melting point, (ii) liquid, and (iii) an intermediate piece with a negative slope that corresponds to a transition from the highest superheated solid state down to the melting curve. The equilibrium melting point ( $P_m, T_m$ ) is then bracketed by ( $P_s, T_s$ ) and ( $P_l, T_l$ ), where the former corresponds to the highest state on the solid part of the crystalline piece, while the latter to the lowest state on the liquid piece, as attained in the AIMD simulations. We take  $P_m = (P_s + P_l)/2$  and  $T_m = (T_s + T_l)/2$  with errors bars  $\Delta P_m = (P_l - P_s)/2$  and  $\Delta T_m = (T_l - T_s)/2$ . The  $Z$  method is described in detail in Ref. [41], where it was developed and carefully tested. It is important to note that the  $Z$  method is different from the so called “heat-until-it-yields” ([42]) method in that the latter does not allow one to eliminate the effect of superheating.

We performed AIMD simulations for a 108-atom ( $3 \times 3 \times 3$  unit cells) fcc system at three volumes: 17.23, 12.66, and  $9.826 \text{ \AA}^3/\text{atom}$ . The corresponding  $P_s$  at high  $T$  (close to  $T_m$ ) are equal to approximately 5, 130, and 400 GPa, respectively. At each volume we performed simulations for

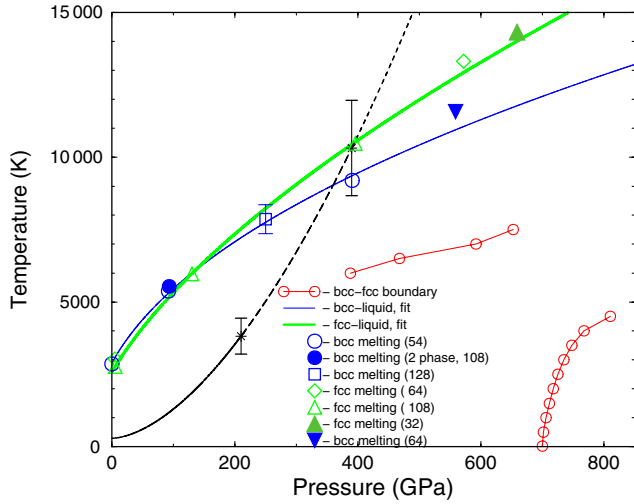


FIG. 2 (color online). Data on the phase stability of Mo. The bcc-fcc phase boundary was constructed using the results shown in Fig. 1. Circles, diamonds, triangles and squares represent melting conditions obtained from AIMD for bcc and fcc Mo; the legend indicates the number of atoms in the AIMD simulation; except one point (bcc, 2-phase method) the  $Z$  method was used. Unless shown explicitly, the error bar is smaller than the size of the corresponding symbol. Our fcc and bcc melting curves obtained from AIMD simulations are shown as solid thick and thin curves, respectively. The two points with temperature error bars are the solid-solid and solid-liquid transitions as measured in shock-wave experiments [2,4]; the corresponding phases on the Hugoniot are shown as a solid curve (bcc phase), long dashed curve (another solid phase), and short-dashed curve (liquid).

several initial  $T$ s in order to closely bracket the  $T_m$ s. The time step in our simulations was 1 fs, and the energy drift with such a small time step was negligible. In each of the simulations equilibrium was achieved in 2500–3000 time steps.  $P$ s were calculated as time averages over additional MD runs of a few hundred time steps performed after the systems had already reached equilibrium. The results of these simulations are shown in Fig. 2. Fitting the well-known Simon form to our 108-atom, AIMD data yields our fcc Mo melting curve ( $P$  in GPa,  $T_m$  in K)

$$T_m(P) = 2585 \left( 1 + \frac{P}{44.0} \right)^{0.61}. \quad (1)$$

The dependence of  $T_m$  on system size was checked by performing additional simulations for both 64-atom (constructed as a  $4 \times 4 \times 4$  60-degree simple rhombohedral cell) and 32-atom ( $2 \times 2 \times 2$  unit cells) fcc systems, at  $17.23 \text{ \AA}^3/\text{atom}$  ( $P \sim 5$  GPa) and  $8.984 \text{ \AA}^3/\text{atom}$  ( $P \sim 570$  GPa), and  $8.582 \text{ \AA}^3/\text{atom}$  ( $P \sim 660$  GPa), respectively. Size effects turn out to be negligible: the low- $P$  108-atom and 64-atom results overlap within uncertainties, and both the high- $P$  64-atom and 32-atom points lie very close to the 108-atom melting curve, Eq. (1); see Fig. 2.

We also performed three AIMD simulations of a 54-atom ( $3 \times 3 \times 3$  unit cells) bcc system, a single simulation of both 64-atom (constructed as a  $4 \times 4 \times 4$  109.5-degree simple rhombohedral cell) and 128-atom ( $4 \times 4 \times 4$  unit cells) bcc systems to check for size effects, and a 2-phase simulation of a 108-atom (54-atom solid plus 54-atom liquid) bcc cell to check for consistency of the  $Z$  and 2-phase methods. Simulations were performed at volumes of  $17.97$ ,  $13.50$ , and  $9.842 \text{ \AA}^3/\text{atom}$  for the 54-atom system,  $8.992 \text{ \AA}^3/\text{atom}$  for the 64-atom system, and  $10.98 \text{ \AA}^3/\text{atom}$  for the 128-atom system. The corresponding  $P$ s are equal to about  $-3$ ,  $90$ ,  $390$ , and  $560$ , and  $250$  GPa, respectively. The 2-phase 108-atom system was simulated at  $13.50 \text{ \AA}^3/\text{atom}$  ( $P \sim 90$  GPa). The results of these simulations are also shown in Fig. 2. They demonstrate that (i) both  $Z$  and two-phase methods are indeed consistent with each other, and (ii) as for fcc, the bcc size effects are negligible. Our bcc melting curve  $T_m(P) = 2894(1 + \frac{P}{35.0})^{0.47}$  is in good agreement with that recently calculated by Cazorla *et al.* [16],  $T_m(P) = 2894(1 + P/37.2)^{0.43}$ , which gives bcc  $T_m$ s  $\sim 10\%$  lower than ours at high  $P$ . Comparison of our fcc and bcc melting curves shows that fcc melts at higher  $T$  than bcc at high  $P$ , which means that it is more stable than bcc, in agreement with our quasiharmonic phonon calculations discussed above.

Using the results of recent shock-wave experiments and previous theoretical studies [43,44], we obtained the following analytic form for the Mo Hugoniot,  $T_H(P) = 293 + 0.424 \cdot P^{1.688}$  (to 5 Mbar), which is shown in Fig. 2, along with the corresponding 16% error bars at the transition  $P$ s of 2.1 and 3.9 Mbar [2].

A linear extrapolation of the high- $T$  bcc-fcc boundary to lower  $P$  passes very close to the bcc-fcc shock-wave point, though it remains somewhat below. We note, however, that the actual bcc-fcc boundary may be lower than that calculated in the quasiharmonic approximation because of anharmonicity. In view of the uncertainty in the estimated  $T$  of the solid-solid transition point on the shock Hugoniot and anharmonic corrections to our calculated bcc-fcc boundary, the agreement between our AIMD-based melting curves, our quasiharmonic bcc-fcc boundary, and the shock-wave data is very good. The solid-solid transition on the Hugoniot might in fact involve a phase more stable than fcc, in which case the transition  $T$  would be lower, as in Fig. 2.

In summary, using well established methods we discovered that the Mo fcc melting curve lies above the bcc one at  $P \gtrsim 1.5$  Mbar, and therefore fcc is more stable than bcc at elevated  $T$  and  $P$ . This is quite consistent with our quasiharmonic calculations for the bcc-fcc boundary, which makes our findings very robust. Other crystal structures may have even higher  $T_m$  than fcc but our work, for the first time, conclusively demonstrates that there is at least one other solid phase above the bcc stability field at high  $P$ .

Computations were performed using the facilities at the Swedish National Infrastructure for Computing (SNIC) and the LANL Coyote cluster. We also wish to thank the Swedish Research Council (VR) and the Swedish Foundation for Strategic Research (SSF) for financial support.

- 
- [1] A. C. Mitchell and W. J. Nellis, *J. Appl. Phys.* **52**, 3363 (1981).
- [2] R. S. Hixson *et al.*, *Phys. Rev. Lett.* **62**, 637 (1989).
- [3] Y. K. Vohra and A. L. Ruoff, *Phys. Rev. B* **42**, 8651 (1990).
- [4] R. S. Hixson and J. N. Fritz, *J. Appl. Phys.* **71**, 1721 (1992).
- [5] A. L. Ruoff, H. Xia, and Q. Xia, *Rev. Sci. Instrum.* **63**, 4342 (1992).
- [6] D. Errandonea *et al.*, *Phys. Rev. B* **63**, 132104 (2001).
- [7] B. K. Godwal and R. Jeanloz, *Phys. Rev. B* **41**, 7440 (1990).
- [8] J. A. Moriarty, *Phys. Rev. B* **45**, 2004 (1992).
- [9] N. Singh, *Phys. Rev. B* **46**, 90 (1992).
- [10] S. M. Foiles, *Phys. Rev. B* **48**, 4287 (1993).
- [11] J. A. Moriarty, *Phys. Rev. B* **49**, 12 431 (1994).
- [12] P. Söderlind *et al.*, *Phys. Rev. B* **49**, 9365 (1994).
- [13] N. E. Christensen, A. L. Ruoff, and C. O. Rodriguez, *Phys. Rev. B* **52**, 9121 (1995).
- [14] Y. Wang, D. Chen, and X. Zhang, *Phys. Rev. Lett.* **84**, 3220 (2000).
- [15] A. B. Belonoshko, S. I. Simak, A. E. Kochetov, B. Johansson, L. Burakovsky, and D. L. Preston, *Phys. Rev. Lett.* **92**, 195701 (2004).
- [16] C. Cazorla, M. J. Gillan, S. Taioli, and D. Alfé, *J. Chem. Phys.* **126**, 194502 (2007).
- [17] A. K. Verma, R. S. Rao, and B. K. Godwal, *J. Phys. Condens. Matter* **16**, 4799 (2004).
- [18] A. B. Belonoshko and L. Dubrovinsky, *Am. Mineral.* **82**, 441 (1997).
- [19] A. B. Belonoshko, R. Ahuja, and B. Johansson, *Phys. Rev. B* **61**, 11 928 (2000).
- [20] A. B. Belonoshko and L. S. Dubrovinsky, *Am. Mineral.* **81**, 303 (1996).
- [21] L. Zhang, Z. Gong, and Y. Fei, in *Proceedings of the AGU Joint Assembly, Baltimore, MD, May 23–26*, No. M34B-01 (AGU, Washington, DC, 2006), unpublished.
- [22] A. Aguado and P. A. Madden, *Phys. Rev. Lett.* **94**, 068501 (2005).
- [23] J. M. Brown and B. G. McQueen, *J. Geophys. Res.* **91**, 7485 (1986).
- [24] A. B. Belonoshko, R. Ahuja, and B. Johansson, *Phys. Rev. Lett.* **84**, 3638 (2000); A. B. Belonoshko, R. Ahuja, and B. Johansson, *Nature (London)* **424**, 1032 (2003).
- [25] L. S. Dubrovinsky *et al.*, *Science* **316**, 1880 (2007).
- [26] A. B. Belonoshko, R. Ahuja, and B. Johansson, *Phys. Rev. Lett.* **87**, 165505 (2001); A. B. Belonoshko *et al.*, *J. Chem. Phys.* **117**, 7233 (2002); A. B. Belonoshko *et al.*, *Phys. Rev. B* **74**, 054114 (2006).
- [27] F. Saija and S. Prestipino, *Phys. Rev. B* **72**, 024113 (2005).
- [28] A. B. Belonoshko, *Geochim. Cosmochim. Acta* **58**, 4039 (1994); A. B. Belonoshko *et al.*, *Phys. Rev. Lett.* **94**, 195701 (2005).
- [29] A. B. Belonoshko, *Geoch. Cosmochim. Acta* **58**, 4039 (1994).
- [30] A. B. Belonoshko, *Phys. Chem. Miner.* **25**, 138 (1998); R. Ahuja, A. B. Belonoshko, and B. Johansson, *Phys. Rev. E* **57**, 1673 (1998).
- [31] L. Vocadlo and D. Alfé, *Phys. Rev. B* **65**, 214105 (2002).
- [32] A. B. Belonoshko *et al.*, *Phys. Rev. B* **61**, 3838 (2000); L. Vocadlo, D. Alfé, G. D. Price, and M. J. Gillan, *J. Chem. Phys.* **120**, 2872 (2004).
- [33] P. E. Blöchl, *Phys. Rev. B* **50**, 17953 (1994); G. Kresse and D. Joubert, *Phys. Rev. B* **59**, 1758 (1999).
- [34] G. Kresse and J. Hafner, *Phys. Rev. B* **48**, 13 115 (1993); G. Kresse and J. Furthmüller, *Comput. Mater. Sci.* **6**, 15 (1996).
- [35] Y. Wang and J. P. Perdew, *Phys. Rev. B* **44**, 13298 (1991); J. P. Perdew *et al.*, *Phys. Rev. B* **46**, 6671 (1992).
- [36] H. J. Monkhorst and J. D. Pack, *Phys. Rev. B* **13**, 5188 (1976).
- [37] M. Methfessel and A. T. Paxton, *Phys. Rev. B* **40**, 3616 (1989).
- [38] P. E. Blöchl, O. Jepsen, and O. K. Andersen, *Phys. Rev. B* **49**, 16 223 (1994).
- [39] G. Kresse and J. Furthmüller, *Europhys. Lett.* **32**, 729 (1995); A. van de Walle and G. Ceder, *Rev. Mod. Phys.* **74**, 11 (2002).
- [40] F. D. Murnaghan, *Proc. Natl. Acad. Sci. U.S.A.* **30**, 244 (1944); F. Birch, *J. Geophys. Res.* **83**, 1257 (1978).
- [41] A. B. Belonoshko, N. V. Skorodumova, A. Rosengren, and B. Johansson, *Phys. Rev. B* **73**, 012201 (2006).
- [42] A. B. Belonoshko, *Am. Mineral.* **86**, 193 (2001).
- [43] V. W. Yuan *et al.*, *Phys. Rev. Lett.* **94**, 125504 (2005), and references therein.
- [44] D. C. Swift, A. Seifert, D. B. Holtkamp, and D. A. Clark, *Phys. Rev. B* **76**, 054122 (2007).